Frontiers of Information Technology & Electronic Engineering
www.zju.edu.cn/jzus; engineering.cae.cn; www.springerlink.com
ISSN 2095-9184 (print); ISSN 2095-9230 (online)
E-mail: jzus@zju.edu.cn

New technique:

Design and calibration of a new high-definition three-dimensional laparoscopic system*

Jia TANG, Li-qiang WANG†‡, Bo YUAN, Hong JIANG, Qi-ming ZHU

(*State Key Laboratory of Modern Optical Instrumentation, Optical Engineering Department, Zhejiang University, Hangzhou 310027, China*)

†E-mail: wangliqiang@zju.edu.cn

Received Apr. 22, 2014; Revision accepted Sept. 25, 2014; Crosschecked Dec. 8, 2014

Abstract: We present a high-definition (HD) 3D laparoscopic system including a dual channel optical system, two cameras, a camera control unit (CCU), and an HD 3D monitor. This laparoscopic system is capable of outputting dual high-definition videos and providing vivid 3D images. A modified pinhole camera model is used for camera calibration and a new method of depth measurement to improve precision. The average error of depth measurement measured by experiment (about 1.13 mm) was small in proportion to the large range in distance of the system (10–150 mm). The new method is applicable to any calibrated binocular vision system.

Key words: Dual optical channels, Three dimensional, Camera calibration, Pinhole model, Depth measurement, Laparoscopic system

doi:10.1631/FITEE.1400149 **Document code:** A **CLC number:** TP391; R608

1 Introduction

Minimally invasive surgery (MIS) has been changing the way people think about surgery. Patients who choose these innovative procedures over conventional surgery usually have a shorter hospital stay and a quicker recovery. To perform laparoscopic surgery, surgeons require specially designed thin instruments and a laparoscope. During the surgery, one of the most important challenges surgeons have had to face has been the loss of depth perception because of the 2D vision of laparoscopic cameras. Many studies of 2D and 3D laparoscopes have concluded that a 3D laparoscopic system with more accurate depth perception may improve the efficiency, shorten the learning curve, and reduce the operating time of the surgery (Feng *et al.*, 2010; Honeck *et al.*, 2012).

Because of the perceived need for and potential benefits of 3D laparoscopes, many medical imaging equipment manufacturers have developed related technology and products. InnerOptic Technology Inc. (Keller and State, 2011) developed a single-image stereoscopic laparoscope, which is a dual channel optical system that can be mounted on a single conventional high-definition (HD) camera head. This product is used to upgrade a conventional HD laparoscopic system to a 3D system. It reduces the cost of upgrading, but half of the image resolution is lost. Seoul National University Hospital also produced a 3D laparoscope, which uses a one-camera mechanism to change the path of light using the difference in density between objects (Kong *et al.*, 2009). The one-camera system splits the natural light into two polarized beams representing the left and right views

‡ Corresponding author

* Project supported by the National Key Technology R&D Program of China (Nos. 2011BAI12B06 and 2012BAI14B06) and the Fundamental Research Funds for the Central Universities, China (No. 2013FZA5018)

ORCID: Jia TANG, http://orcid.org/0000-0001-9873-2733; Li-qiang WANG, http://orcid.org/0000-0002-9940-4480

of the object. Using this method, the illumination of the one-camera system will be only half that of a conventional binocular system with the same light source. Recently, the Olympus Corporation has released its newest 3D laparoscopic system, the Endoeye Flex 3D system (Edgcumbe *et al.*, 2013). This system includes a dual lens system with two high-resolution charge-coupled device (CCD) image sensors. The sensors are located at the distal end of the laparoscope to provide the left and right images, respectively. The tip of system can bend up to 100° in four directions, so it has a wider field of view than a conventional laparoscope with only front view. This angular flexibility facilitates surgical techniques that make the most of the space available, even during technically difficult procedures.

In this article, we introduce a new 3D laparoscopic system, which includes a dual channel optical system, two cameras, a camera control unit (CCU), and a 3D monitor. Each optical channel has an 80° field of view and less than 3% distortion, and the Nyquist frequency matches the pixel size of the CMOS sensor. By mounting two CMOS sensors behind the relay lenses of the laparoscope, we are able to avoid image degradation caused by the triangular prism and thereby obtain a higher quality image. The modified system also has the advantage of being compact. The HD optical system and matching camera system represent a new 3D laparoscope.

2 HD optical system

The HD optical system, including two parallel optical channels assembled in a tube of 10-mm diameter and 335-mm length, is shown in Fig. 1. Each optical channel contains an objective lens and five relay lenses. The objective and relay lenses in the channel are in line and on the axis. The objective lens is straight with no convergence, with a field of view of 80°. The relay lenses with unit magnification are a modified Hopkins rod-lens system (Ellis, 2007).

Based on the pixel size of the chosen CMOS (1.75 μm×1.75 μm) and the required field of view, the effective focal length of the objective optics is designed to be 1.66 mm. The relay lenses comprise four doublet rod lenses arranged end to end on a common optical axis. They make no contribution to the

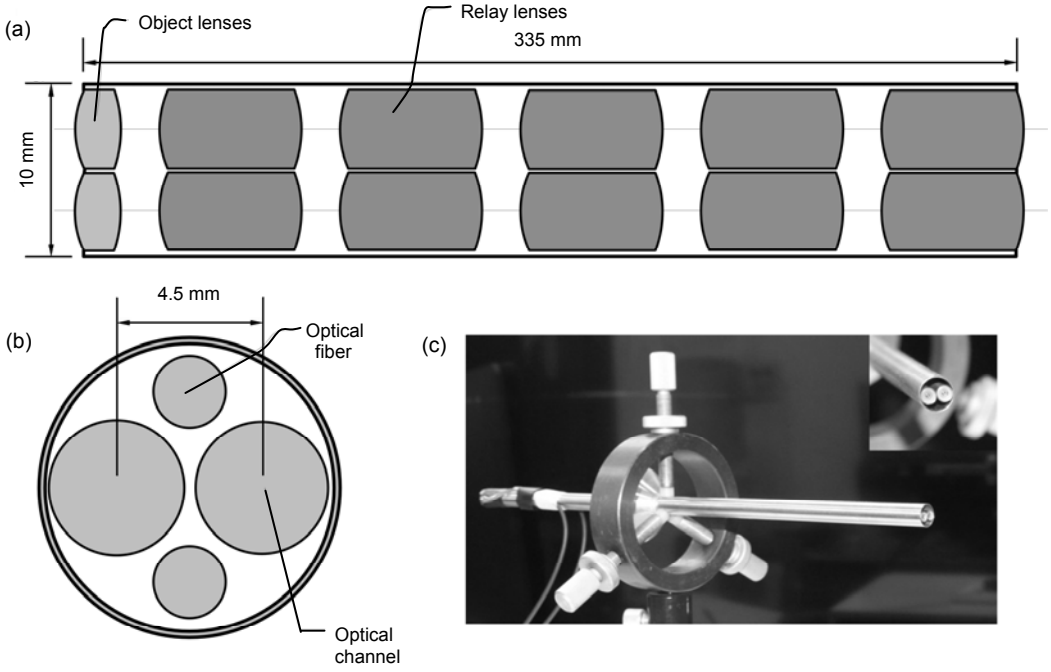

Fig. 1 The optical system of the 3D laparoscope

(a) A view of the optical system including two optical channels; (b) Arrangement of optical cores; (c) A real image of the dual channel optical system

effective focal length, so the focal length of the whole optical system is equal to the focal length of the objective optics. The total track of the system is 335 mm, and the lens *f*-number is 4.74.

3 Camera calibration

Camera calibration is a necessary step in 3D computer vision to extract metric information from 2D images. The primary purpose of camera calibration is to find the internal properties of the camera that affect the imaging process. Much work has been done, first in photogrammetry, and more recently in computer vision. The pinhole model is usually considered as the camera model for calibration (Heikkila and Silven, 1997; Zhang, 2000), and can simplify the calibration procedure. Some studies (Wengert *et al.*, 2006; Barreto *et al.*, 2009; Melo *et al.*, 2012) in camera calibration of endoscopes also used the pinhole camera model. Bouguet (2013) presented a popular application for camera calibration. In the pinhole camera model, the distance between the image plane and optical center is the focal length f', which means that the image plane is the focus plane. This hypothesis is accurate only in the condition that the working distance is far longer than the focal length, which limits the application of the pinhole model.

The working distance of a general laparoscope of 10–150 mm is not infinite, and is also not much longer than the focal length of the optical system, so the pinhole camera model cannot be applied to real laparoscope calibration. It needs to be adjusted.

The best solution for calibrating our laparoscope is classical geometrical optics. Fig. 2 shows the geometry of the pinhole camera. Suppose that the focal length of the camera is f, and that the working distance is l. The image distance l' can be calculated from

$$l' = \frac{f'l}{f' + l}. \tag{1}$$

Using nf (n is a positive number greater than 1, $f=-f'$) instead of l, Eq. (1) is transformed to

$$l' = \frac{nf'}{n-1}. \tag{2}$$

In the pinhole model, the working distance nf is long enough and $n/(n-1)$ is close to 1, as can be seen from Eq. (2) . Then Eq. (2) can be substituted by

$$l' \approx f'. \tag{3}$$

Thus, the image plane can also be called the focus plane in the pinhole model.

In the laparoscope situation where the working distance is much shorter, the parameters of the optical system are designed according to the best working distance of 40 mm. The focal length is 1.66 mm, and the calculated image distance is 1.74 mm. So, in our laparoscope situation, the image distance (l') is $1.042f'$, not f'. This 4.2% change in image distance has a significant impact on the following experiment in depth perception. The results of calibration are shown in Table 1.

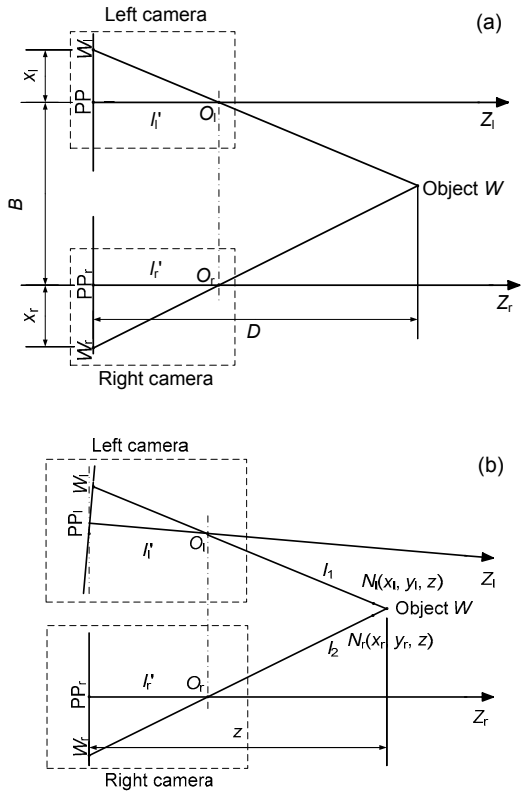

Fig. 2 Ideal (a) and real (b) camera models of the laparoscope

O_l (O_r) represents the optical center of the left (right) camera; PP_l (PP_r) represents the principal point of the left (right) camera; W_l (W_r) is the left (right) imaging point of object W

Table 1 The main characteristics of the laparoscope

Parameter	Left camera	Right camera
Focal length (mm)	1.664	1.673
Principle point (pixel)	(695.7, 455.2)	(681.8, 418.9)
Translation vector (pixel)	(4.43839, 0.86019, 0.14590)	
Rotation vector (pixel)	(−0.00480, −0.00398, −0.00088)	

4 Distance measurement experiment

A distance measuring experiment was designed to check the accuracy of depth perception. The laparoscope was used to capture binocular images of the target at different depths between 10 mm and 150 mm at a pitch of 5 mm. A widely used algorithm for distance measurement is traditional stereo triangulation (Field *et al.*, 2009), which is based on the similar triangle principle. The distance of an object can be easily obtained according to triangle similarity:

$$D=1.042f\cdot\left(1+\frac{B}{x_\mathrm{l}+x_\mathrm{r}}\right), \tag{4}$$

where $x_\mathrm{l}+x_\mathrm{r}$ is the parallax between the left and right images, B is the baseline between the cameras, and f is the focal length of the cameras (Fig. 2a).

To obtain accurate data from stereo triangulation, the image planes of the right and left cameras should be as coincident as possible. However, in reality the camera model for laparoscopy is more like that shown in Fig. 2b. In this situation, using the stereo triangulation algorithm may increase unexpected errors.

With this concern, we present a new method to measure the depth. The fundamental principle of the new method is to consider two straight lines intersecting at one point. After calibration and some transformation of coordinates, the coordinates of the left and right cameras can be transformed into the same coordinates (Fig. 2b). We define line l_1 as the line that crosses the left image point W_l and the left camera's optical center O_l, and line l_2 as the line that crosses the right image point W_r and the right camera's optical center O_r. Ideally, lines l_1 and l_2 should intersect at the object point W (Fig. 2b). However, considering the system error, these two lines may not intersect. So, we use the position where the distance between the two lines is shortest instead of the point of intersection. The coordinates of W_r, O_r, W_l, and O_l are known after camera calibration and transformation, and the lines l_1, l_2 are determined by W_r, O_r, W_l, and O_l.

For example, consider an object point $W(x, y, z)$ with two image points $W_\mathrm{l}(x_1, y_1, z_1)$ and $W_\mathrm{r}(x_2, y_2, z_2)$, with known coordinates of $O_\mathrm{l}(x_3, y_3, z_3)$ and $O_\mathrm{r}(x_4, y_4, z_4)$. The lines l_1 and l_2 can be expressed as

$$l_1:\frac{x-x_1}{x_3-x_1}=\frac{y-y_1}{y_3-y_1}=\frac{z-z_1}{z_3-z_1}, \tag{5}$$

$$l_2:\frac{x-x_2}{x_4-x_2}=\frac{y-y_2}{y_4-y_2}=\frac{z-z_2}{z_4-z_2}. \tag{6}$$

After several steps of transformation, Eqs. (5) and Eq. (6) turn into Eqs. (7) and (8), respectively:

$$l_1:\begin{cases}x=\dfrac{x_3-x_1}{z_3-z_1}\cdot z+\left(x_1-\dfrac{x_3-x_1}{z_3-z_1}\cdot z_1\right),\\ y=\dfrac{y_3-y_1}{z_3-z_1}\cdot z+\left(y_1-\dfrac{y_3-y_1}{z_3-z_1}\cdot z_1\right),\end{cases} \tag{7}$$

$$l_2:\begin{cases}x=\dfrac{x_4-x_2}{z_4-z_2}\cdot z+\left(x_2-\dfrac{x_4-x_2}{z_4-z_2}\cdot z_2\right),\\ y=\dfrac{y_4-y_2}{z_4-z_2}\cdot z+\left(y_2-\dfrac{y_4-y_2}{z_4-z_2}\cdot z_2\right).\end{cases} \tag{8}$$

Then using Eqs. (9) and (10) to simplify Eqs. (7) and (8), we obtain Eqs. (11) and (12):

$$\begin{cases}a_1=\dfrac{x_3-x_1}{z_3-z_1},\ b_1=x_1-\dfrac{x_3-x_1}{z_3-z_1}\cdot z_1,\\ c_1=\dfrac{y_3-y_1}{z_3-z_1},\ d_1=y_1-\dfrac{y_3-y_1}{z_3-z_1}\cdot z_1,\end{cases} \tag{9}$$

$$\begin{cases}a_2=\dfrac{x_4-x_2}{z_4-z_2},\ b_2=x_2-\dfrac{x_4-x_2}{z_4-z_2}\cdot z_2,\\ c_2=\dfrac{y_4-y_2}{z_4-z_2},\ d_2=y_2-\dfrac{y_4-y_2}{z_4-z_2}\cdot z_2,\end{cases} \tag{10}$$

$$l_1:\begin{cases}x=a_1z+b_1,\\ y=c_1z+d_1,\end{cases} \tag{11}$$

$$l_2:\begin{cases}x=a_2z+b_2,\\ y=c_2z+d_2.\end{cases} \tag{12}$$

The distance between point $N_l(x_l, y_l, z)$ on line l_1 and point $N_r(x_r, y_r, z)$ on line l_2 with the same coordinate z can be expressed as

$$d=\sqrt{(x_1-x_2)^2+(y_1-y_2)^2}. \tag{13}$$

According to Eqs. (11) and (12), using z instead of x_1, y_1, x_2, y_2, the above equation becomes

$$\begin{aligned} d&=\sqrt{[(a_1-a_2)z+(b_1-b_2)]^2+[(c_1-c_2)z+(d_1-d_2)]^2}\\ &=\{[(a_1-a_2)^2+(c_1-c_2)^2]z^2+2[(a_1-a_2)(b_1-b_2)\\ &\quad+(c_1-c_2)(d_1-d_2)]z+(b_1-b_2)^2+(d_1-d_2)^2\}^{1/2}. \end{aligned} \tag{14}$$

The distance d reaches minimum when

$$z=-\frac{(a_1-a_2)(b_1-b_2)+(c_1-c_2)(d_1-d_2)}{(a_1-a_2)^2+(c_1-c_2)^2}. \tag{15}$$

In Eq. (15) z is also the distance measured between the cameras and the object.

Then we do a series of distance measurement experiments and gather the data for distances between 10 mm and 150 mm at a pitch of 5 mm. We use the traditional stereo triangulation algorithm and the new algorithm to calculate the distance. The errors of these two algorithms are shown in Fig. 3.

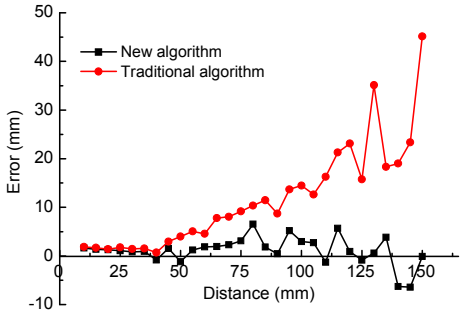

Fig. 3 Error curves of distance measurement

It is observed that the error increases as the distance increases under the traditional stereo triangulation method. For example, at an actual depth of 150 mm, the error of the experiment is about 45 mm, which is too large to be acceptable. So, stereo triangulation is not suitable for our laparoscopic system.

The maximum error under our new method is below 6 mm and the average error is about 1.13 mm. The experimental results demonstrate the feasibility of our new method.

5 Whole package of the HD 3D laparoscopic system

The HD 3D laparoscopic system (Fig. 4) includes a dual channel optical system, two cameras, a camera control unit (CCU), and an HD 3D monitor. Each channel of the optical system has an 80° field of view and less than 3% distortion, and the Nyquist frequency of the optical channel matches the pixel size of the COMS sensor. The CCU, equipped with an i7 CPU and two high-speed data acquisition cards, can provide sufficient bandwidth for storage, transmission, and real-time processing of data. The CCU is also capable of real-time video image processing and display. With dual 720p video inputs, it provides an output of 1080p 3D video by HDMI.

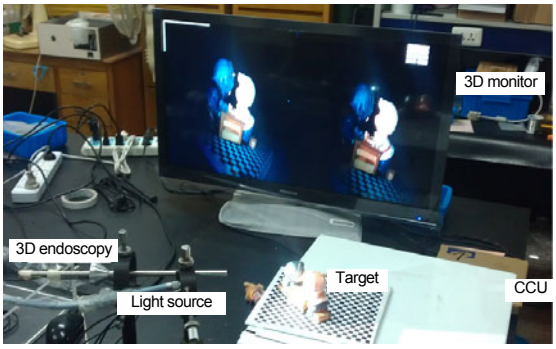

Fig. 4 Brief view of the whole system of the 3D laparoscope

6 Conclusions

In the present study, we have presented a high-definition 3D laparoscope, which has dual optical channels, two cameras, a 3D camera control unit (CCU), and a 3D monitor. The system has high optical performance including an 80° field of view and less than 3% distortion. The specially designed CCU can provide real-time video image processing, display, and 1080p HD HDMI output. Compared with one-camera 3D laparoscope systems, our 3D laparoscope with binocular vision has a more simple structure.

Usually, one-camera 3D laparoscope systems contain reflexed mirrors and require more complicated algorithms to process the images. Compared with Olympus's Endoeye Flex 3D, our 3D laparoscope is less expensive and more convenient in terms of portability.

To check the performance of the 3D laparoscope, a series of depth perception experiments were carried out after camera calibration. We presented a new way to measure the depth, based on two straight lines l_1, l_2 intersecting at an object point. After calibration, the coordinates of the optical centers can be calculated and the coordinates of the image points are easy to obtain. The average error of the depth measurement in the experiments was about 1.13 mm. This error was less than that of stereo triangulation.

References

Barreto, J.P., Roquette, J., Sturm, P., *et al*., 2009. Automatic camera calibration applied to medical endoscopy. Proc. 20th British Machine Vision Conf., p.1-10. [doi:10.5244/C.23.52]

Bouguet, J.Y., 2013. Camera Calibration Toolbox for Matlab. Available from http://www.vision.caltech.edu/bouguetj/calib_doc/ [Accessed on July 30, 2014].

Edgcumbe, P., Nguan, C., Rohling, R., 2013. Calibration and stereo tracking of a laparoscopic ultrasound transducer for augmented reality in surgery. Proc. 6th Int. Workshop on Augmented Reality Environments for Medical Imaging and 8th Int. Workshop on Computer-Assisted Interventions, p.258-267. [doi:10.1007/978-3-642-40843-4_28]

Ellis, H., 2007. The Hopkins rod-lens system. *J. Perioper. Pract.*, **17**(6):272-274.

Feng, C., Rozenblit, J.W., Hamilton, A.J., 2010. A computerized assessment to compare the impact of standard, stereoscopic, and high-definition laparoscopic monitor displays on surgical technique. *Surg. Endosc.*, **24**(11):2743-2748. [doi:10.1007/s00464-010-1038-6]

Field, M., Clarke, D., Strup, S., *et al*., 2009. Stereo endoscopy as a 3-D measurement tool. Proc. Annual Int. Conf. of the IEEE Engineering in Medicine and Biology Society, p.5748-5751. [doi:10.1109/IEMBS.2009.5332606]

Heikkila, J., Silven, O., 1997. A four-step camera calibration procedure with implicit image correction. Proc. IEEE Computer Society Conf. on Computer Vision and Pattern Recognition, p.1106-1112. [doi:10.1109/CVPR.1997.609468]

Honeck, P., Wendt-Nordahl, G., Rassweiler, J., *et al*., 2012. Three-dimensional laparoscopic imaging improves surgical performance on standardized ex-vivo laparoscopic tasks. *J. Endourol.*, **26**(8):1085-1088. [doi:10.1089/end.2011.0670]

Keller, K., State, A., 2011. A single-imager stereoscopic endoscope. SPIE, **7964**:79641Z.1-79641Z.6. [doi:10.1117/12.873011]

Kong, S.H., Oh, B.M., Yoon, H., *et al*., 2009. Comparison of two- and three-dimensional camera systems in laparoscopic performance: a novel 3D system with one camera. *Surg. Endosc.*, **24**(5):1132-1143. [doi:10.1007/s00464-009-0740-8]

Melo, R., Barreto, J.P., Falcao, G., 2012. A new solution for camera calibration and real-time image distortion correction in medical endoscopy—initial technical evaluation. *IEEE Trans. Biomed. Eng.*, **59**(3):634-644. [doi:10.1109/TBME.2011.2177268]

Wengert, C., Reeff, M., Cattin, P.C., *et al*., 2006. Fully automatic endoscope calibration for intraoperative use. Proc. des Workshop on Algorithmen Systeme Anwendungen, p.419-423. [doi:10.1007/3-540-32137-3_85]

Zhang, Z., 2000. A flexible new technique for camera calibration. *IEEE Trans. Patt. Anal. Mach. Intell.*, **22**(11):1330-1334. [doi:10.1109/34.888718]